# Study on adhesion strength, thermal creep resistance, and light transmittance of ethylene-polypropylene copolymer grafted with silane for photovoltaic application

**Joonho Kim,[1] Hwi Yong Lee,[1] Ju Young Park,[2] Youn Cheol Kim,[2] Younggon Son[2]**

[1]Innox Corporation, 171 Asan-Valley Rd, Asan, Chungnam, 336871, South Korea
[2]Division of Advanced Materials Science and Engineering, Kongju National University, Cheonan, Chungnam, 331717, South Korea
Correspondence to: Y. Son (E-mail: sonyg@kongju.ac.kr)

**ABSTRACT:** We investigated the possibility of using PP as an encapsulant in a photovoltaic module. PP is inexpensive but shows low adhesion strength to glass (and silicon wafer) due to its nonpolar nature as well as opacity due to its crystalline nature. We resolved these problems by employing metallocene catalyzed ethylene-propylene copolymer (EPR) and a nucleating agent to increase the transparency. Five EPRs having various propylene/ethylene ratios were investigated. EPRs having higher propylene content showed higher adhesion strength to the glass substrate. However, it is not appropriate to use EPRs with higher propylene content because they show low processability in calendaring processing. We therefore used a blend of two EPRs. The blend of the two EPRs showed somewhat low transparency. When the nucleating agent was incorporated in the blend, the transparency was remarkably increased. The adhesion strength to the glass plate was enhanced by a silane coupling agent. © 2016 Wiley Periodicals, Inc. J. Appl. Polym. Sci. **2016**, *133*, 43464.

## INTRODUCTION

The solar energy market has experienced unprecedented growth in recent decades due to many problems such as the impending exhaustion of fossil fuels, global warming, radiation leaks at Fukushima, difficulties in radioactive waste disposal, etc. Many countries provide financial support to this fledgling industry and research funds to R&D institutes researching solar energy.[1,2] A photovoltaic (PV) module consists of a protective glass on the front face, an encapsulant layer, silicone PV cells, another encapsulant layer, and a back sheet on the rear side. The encapsulant enhances the durability of the module by preventing direct contact between the glass and the silicon wafer and its role has become increasingly important. The encapsulant must be highly transparent, an electrical insulator, inexpensive, and elastomeric. It must have low water permeability and high creep resistance at an elevated temperature. Its adhesion strength to the glass, solar cell, and back sheet must be sufficiently high.

EVA (ethylene vinyl acetate) is the most commonly employed encapsulant material to fulfil those requirements. EVA has a low melting point and does not have high thermal creep resistance. To increase the creep resistance, EVA is cross-linked by an incorporated curing agent during a lamination process.[3–6] However, this curing process causes two major problems. First, the

total time for manufacturing the PV module becomes long, typically over 20 minutes, due to the long curing time. Accordingly, the manufacturing cost is increased. Second, since total cross-linking is not fully achieved, the peroxide used as the cross-linking agent is not completely consumed and the remaining peroxide promotes oxidation and degradation of the EVA encapsulant,[7,8] thus exacerbating EVA's inherent weakness against oxidation and degradation.[9–13] Degradation of the encapsulant can cause discoloration and lead to light transmission losses and delamination, which significantly reduce the durability of the module.[14] An enormous body of research on EVA as an encapsulant for PV modules has been produced and the major topic of investigation is the degradation of EVA.[15]

Other polymers have been explored to overcome this limit. Besides EVA, polar ethylene copolymers such as poly(ethylene-*r*-acrylic acid),[16] polyvinylbutyral,[17] ethylene(methylacrylate), ethylene(ethylacrylate), and ethylene(butylacrylate) have been investigated.[9–11,18,19] Although these copolymers show somewhat higher thermal stability than EVA, they still display similar shortcomings to those of EVA originating from the polar side group.

Ionomers, thermoplastic polyurethane, polyvinylchloride (PVC), metallocene-catalyzed linear low density polyethylenes, polyolefin

**Table I.** Characteristics of polymers used in this study

| Sample code | Grade name | $C_2$[a] wt % (mol %) | VST[b] | MFI[c] | $\rho$[d] | LT[e] (%) (StDev) | TCR[f] (%/h) | AS[g] (N/cm) |
|---|---|---|---|---|---|---|---|---|
| EPR15 | 6202FL | 15 (20.9) | 47.2 | 9.1 | 0.863 | 98.8 (1.06) | 0 | 9.4 |
| EPR16 | 6101FL | 16 (22.2) | 57.2 | 1.4 | 0.862 | 98.7 (1.38) | 0 | 3.0 |
| EPR11-L | 3000 | 11 (15.6) | 65.6 | 3.6 | 0.873 | 97.4 (1.97) | 2560 | 3.5 |
| EPR11-H | 3020FL | 11 (15.6) | 68.3 | 1.1 | 0.874 | 98.4 (1.85) | 1750 | 0 |
| EPR9 | 3980FL | 9 (12.9) | 76.7 | 3.7 | 0.878 | 96.5 (1.42) | 6 | 0 |

[a] Ethylene content.
[b] Vicat softening temperature (°C).
[c] Melt flow index (g/10 min) under 2.16 kg load at 190 °C.
[d] Density (g/cm$^3$).
[e] Average light transmittance of pristine polymer at 400–700 nm and standard deviation (StDev.).
[f] Thermal creep resistance test at 100 °C for 500 h.
[g] Adhesion strength.

block elastomers, silicone elastomers, and epoxy resins have also been studied as replacements for EVA.[20–23] These polymers are developed based on multicomponent compositions instead of being used independently. For example, Maruyama et al. in Japanese Patent No. JP S56-116047 disclosed a bi-layer encapsulant where the first layer is derived from EVA with a low VA content (20 wt % or lower), polyethylene, or soft PVC and the second layer is derived from an ionomer or EVA with high VA content (20 wt % or higher).

In this study, we present the first investigation on the random PP (containing small amounts of ethylene unit) as an encapsulant in a PV module. PP is inexpensive but shows low adhesion strength to glass (and silicon wafer) due to its nonpolar nature as well as opacity due to its crystalline nature. We resolved these problems by employing a metallocene catalyzed ethylene-propylene copolymer and incorporating a nucleating agent to increase the transparency. To increase the adhesion strength, a silane coupling agent (SCA) was grafted to the PP main chain. Grafting of the SCAs has been employed to enhance the adhesion of polyolefin to natural fibers[24] and inorganic fillers such as mica[25] and talc.[26] Several coupling agents were investigated and the effect of the chemical structure on the adhesion strength was discussed.

## EXPERIMENTAL

### Materials

The polymers used in this study were poly(ethylene-$r$-propylene) (EPR) prepared with a metallocene catalyst by ExxonMobile Corporation. The characteristics of the polymers are summarized in Table I. Ethylene content, melt flow index, Vicat softening temperature, and density were provided by ExxonMobile. The coupling agents investigated in this study were purchased from Shin-Etsu Chemical Co. Ltd, Japan. Characteristics of the SCAs are summarized in Table II. t-Butyl peroxy-2-ethyl-hexyl monocarbonate was used as a radical initiator. It was obtained from Dongbo Chemicals, Korea. The antioxidant used was dilauryl thiodipropionate from Songwon Chemical Co., Korea The nucleating agent was 1,3:2,4-bis-O-[(4-methylphenyl)methylene] hexitol (from Dongbo Chemicals, Cas No. 93379-37-4. IUPAC name is 1-(2,6-bis(4-tolyl)−1,3-diox-

ano(5,4-d)−1,3-dioxan-4-yl)ethane-1,2-diol). Potassium permanganate ($KMnO_4$) and sulphuric acid ($H_2SO_4$) were purchased from Samchun Chemicals, Korea.

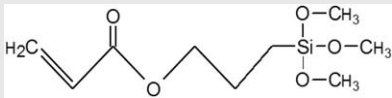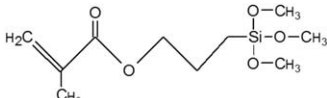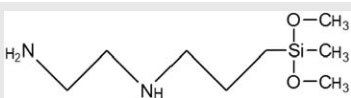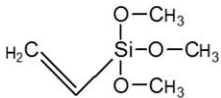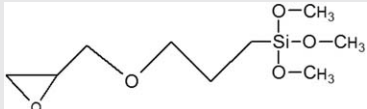### Preparation of the Polymer/Additive Blend

Grafting of the SCA onto EPR was carried out in a twin screw extruder with the aid of a radical initiator. Prior to compounding, all the raw materials were dried in a vacuum oven at 80 °C for a minimum of 12 h. 100 g of EPRs was tumble-mixed with a radical initiator of 0.06 g, antioxidant of 0.2 g, and various amounts of the SCA in a sealed polyethylene bag. The mixture was put into the hopper of the twin screw extruder for compounding. Melt compounding was performed using an intermeshing, co-rotating twin-screw extruder (L/D = 40, $\phi$ = 11 mm, Bautek, Korea) at 180 °C with a screw speed of 200 rpm.

### Characterization

Sheets with thickness of 0.5 mm were prepared by compression molding. Pellets were sandwiched between polyimide films and preheated at 180 °C under minimal pressure for 10 min and then compressed at 10 MPa for 5 min using a Model QM900M laboratory press, Qmesys (Seoul, Korea). Rectangular sheets (70 mm × 50 mm) were cut from the compression molded sheets. The polymer sheet was placed between two glass plates and the sandwiched sample was prepared in a vacuum assisted laminating machine (ARRON ARLA 0505, Korea). The operating temperature and the pressure were 120 °C and 0.1 MPa. A fixture for the creep resistance test was prepared with an additional glass plate and epoxy cement, as shown in Figure 1. 1.0 kg load (equivalent shear stress of 0.28 MPa) was applied vertically. The fixture was placed in an air circulating oven maintained at 100 °C for 500 h. The moving glass goes downward with time as the encapsulant films are flowing. The thermal creep resistance was defined as shear strain [$\gamma(\%) = 100\delta/h$] of deforming encapsulant divided by time [$\Delta t(\mathrm{hr})$]. It is therefore $100\delta/(h\Delta t)$ and the unit is %/h.

A Jasco V-570 UV/vis/NIR spectrophotometer was employed to study the light transmittance of the encapsulant films. The films were sandwiched between two glass slides to prevent curving, and then placed between the light source and the light detector.

**Table II.** Characteristics of SCAs investigated in this study

| Grade | Chemical name | Chemical formula | Adhesion strength[a] (N/cm) |
|---|---|---|---|
| KBM 5103 | 3-Acryloxypropyl trimethoxysilane | | 74 |
| KBM503 | 3-Methacryloxypropyl trimethoxysilane | | 21 |
| KBM602 | N-2-(Aminoethyl)−3-aminopropylmethyldimethoxysilane | | 0 |
| KMB1003 | Vinyltrimethoxysilane | | 33 |
| KMB403 | 3-Glycidoxypropyl trimethoxysilane | | 0 |
| KMB1083 | Octenyltrimethoxysilane | | 0 |

[a] Adhesion strength of EPR15 with 1 phr. of coupling agent.

The transmitted intensity at 400-700 nm wave length was taken to calculate the average light transmission.

Adhesion strength between the glass plate and the polymer sheet was measured according to ASTM D 3330 (peel adhesion testing-180° angle). A 70 mm × 50 mm polymer sheet and a glass plate of the same size were stacked. At the edge of the stack, a Teflon film was inserted between the polymer and the glass to facilitate opening the glass/polymer interface. About 1/7th glass–polymer contact was prevented by the Teflon film. The sandwiched sample was placed in a vacuum assisted laminating machine maintained at 120 °C. A vacuum was established within 3 minutes and pressure of 0.1 MPa was applied on the sample for 8 minutes. After complete adhesion between the glass and the polymer was obtained, the samples were cut into strips of 70 cm × 10 cm. A 180° peel test was carried out in a universal testing machine (Qmesys QM100T, Korea) at a cross head speed of 50 mm/min.

A thermal analysis was performed with a Perkin-Elmer (Boston, MA) DSC-7 calorimeter under a nitrogen atmosphere. Samples weighing 5–10 mg were cut from the molded sheets. Each sample was heated to 130 °C at a rate of 20 °C/min and held for 5 min to remove the residue thermal history. The sample was then quenched to 25 °C, isothermally crystallized for 15 min, and quenched to −50 °C. Heating thermograms was obtained from −50 °C to 130 °C at a rate of 20 °C/min. For cooling scan, samples were melted at 130 °C for 5 min, and a cooling scan was performed from 130 °C to −50 °C with a cooling rate of −20 °C/min.

Compression molded EPR9, EPR15/EPR9(5/5) and EPR15/EPR9(5/5)-Nu0.5 samples were quenched in liquid nitrogen. Fracture surfaces of the samples were prepared in liquid nitrogen and etched in 7 wt % solution of potassium permanganate in sulphuric acid for 15 min at 60 °C. The fracture surface was then platinum-coated. The size of the spherulites were observed in a scanning electron microscope (SEM, a JEOL JSM-6335F).

## RESULTS AND DISCUSSION

### Light Transmittance of Pristine mEPRs

PP cannot be used as an encapsulant in PV modules because it blocks sunlight due to its high crystallinity. Since copolymerization reduces the crystallinity and increases the transparency, we chose poly(propylene-r-ethylene) (ethylene-propylene random copolymer, EPR) as a candidate for the encapsulant. There are fundamental limitations in Ziggler-Natta catalyst to reduce the crystallinity of PP because of a non-uniform comonomer distribution in Ziggler-Natta catalyzed polyolefin.[27] On the other hand, a metallocene catalyst produces polyolefin with a uniform comonomer distribution and provides much lower crystallinity compared to ZN catalyst. Therefore, we investigated metallocene catalyzed EPR (mEPR). Figure 2 shows the transmittance spectra of five different mEPRs having various ethylene comonomer content. In Table I, the average transmittance values at the wavelength of visible light (400–700 nm) together with other properties are summarized. Pristine EPRs showed somewhat high light transmittance at 0.5 mm film thickness, which is a typical thickness for a solar cell encapsulant, and five mEPRs showed similar transparency. When the additives (the SCA, the
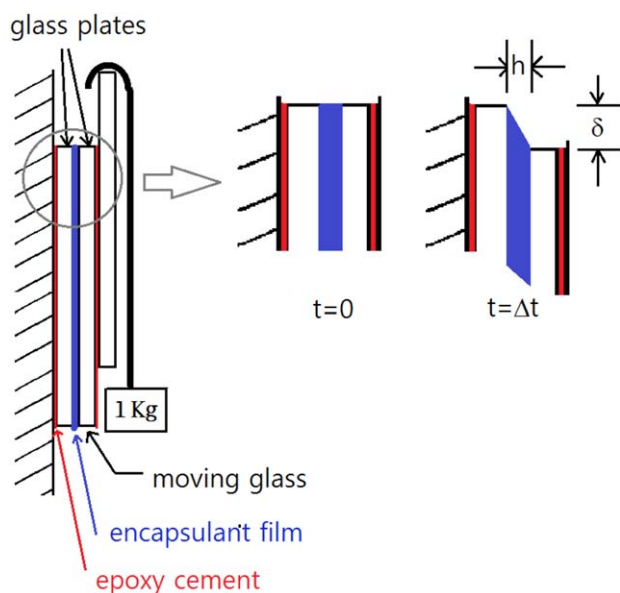
**Figure 1.** Test fixture for thermal creep resistance test. [Color figure can be viewed in the online issue, which is available at wileyonlinelibrary. com.]

initiator, and the antioxidant) were incorporated, the transmittance values decreased. The light transmittance of the mEPR was affected by the ethylene content. It was observed that higher ethylene content (and thus lower crystallinity) leads to higher light transmittance.

### Thermal Creep Resistance

PV modules are operated at elevated temperature due to the continuous exposure to sunlight. Therefore, thermal creep resistance is an important property in the application of PV encapsulants. The thermal creep resistance of mEPRs at 100 °C are summarized in Table I (column f). The thermal creep resistance was defined as shear strain [$\gamma(\%)$] of deforming encapsulant film per hour. It was found that the thermal creep resistance did not follow the order of the softening temperatures and melt flow index. EPR15 showed the lowest softening temperature and the highest MFI (i.e., lowest viscosity), and thus one may naturally expect that its thermal creep resistance would be the lowest.

Figure 3 shows the DSC heating thermograms for the five polymers. All five EPRs showed melting peaks at ∼40 (associated with the $\gamma$ form) and 70 °C ($\alpha$ form).[28,29] It has been reported that PP and its copolymer with $\alpha$-olefin exhibit three different crystallographic forms (monoclinic $\alpha$ form, hexagonal $\beta$ form and orthorhombic $\gamma$ form).[30] The $\beta$ form is found in very rare circumstances such as crystallization under stress or specific nucleating agents. Generally, PP and its copolymer crystallized at normal condition mostly consist of $\alpha$ form and $\gamma$ form.[30] Studies on the polymorphism of PP show that PP exhibits double melting peaks for long crystallization time in isothermal crystallization experiment or at the slow cooling rate in non-isothermal crystallization experiment. By a comparison of the WAXS diffractograms with the DSC thermograms, it was found that the higher temperature peak is attributed to the $\alpha$ form

and the other peak is attributed the $\gamma$ form.[28] EPR15 and EPR16 showed an additional melting peak at ∼100 °C. The EPR15 and EPR16 do not melt completely at 100 °C. For this reason, EPR15 and EPR16 showed the highest creep resistance at 100 °C in spite of their low softening temperature.

### Evaluation of Adhesion Strength for Various Silane Coupling Agent

Table II shows the characteristics of the SCA and the adhesion strength of EPR15 to glass when 1 phr of the SCA was grafted. The alkyl group in SCA reacts with the polyolefin main chain and forms SCA grafted mEPR (mEPR-g-SCA) by aid of the radical initiator in melt grafting process.[31] The methoxy group on the SCA can react with the hydroxyl group on the glass or have a strong physical interaction with the hydroxyl group.[32] As a consequence, mEPR-g-SCA combines strongly mEPR and glass (or silicon wafer) leading to strong adhesion. It was observed that a coupling agent having double bonds provides relatively higher adhesion strength. It is known that peroxide forms radicals, and radicals are formed easily in the double bonds of vinyl,
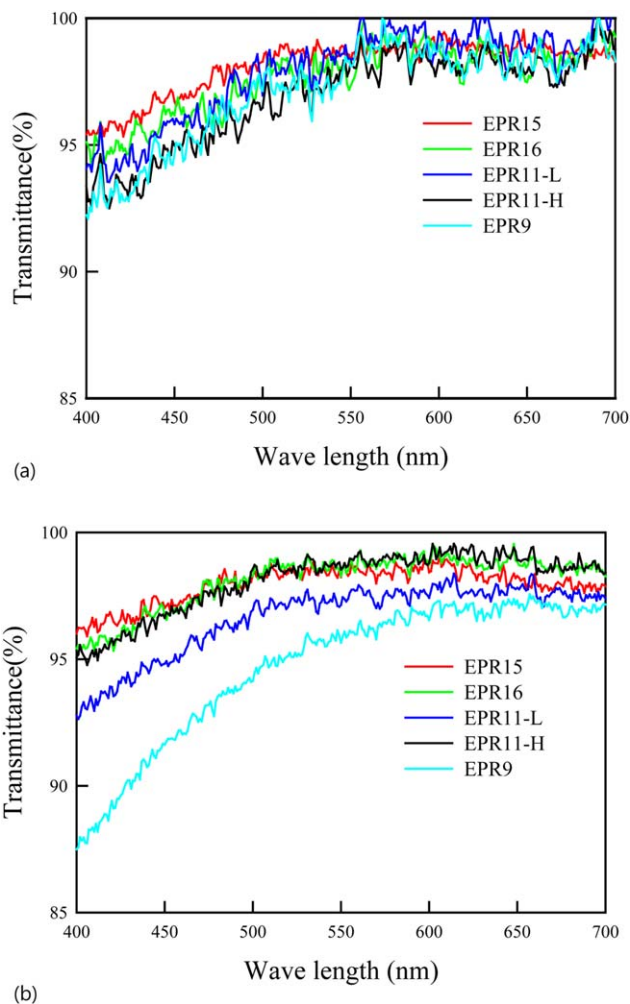


**Figure 2.** Light transmittance spectra of five mEPRs investigated in this study. (a) pristine polymers (b) The polymers were melt-compounded with 1 phr of SCA, 0.06 phr of radical initiator and 0.2 phr of antioxidant. [Color figure can be viewed in the online issue, which is available at wileyonlinelibrary.com.]
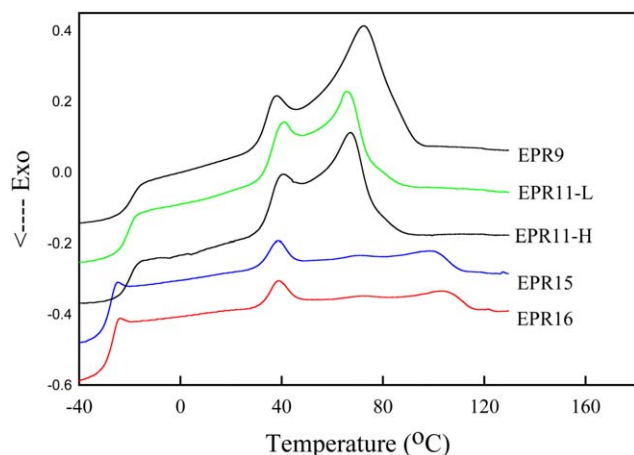
**Figure 3.** DSC heating endotherms for five polymers. The sample was iso-thermally crystallized at 25 °C for 15 min and quenched to −50 °C before heating to 130 °C at a rate of 20 °C/min. [Color figure can be viewed in the online issue, which is available at wileyonlinelibrary.com.]

acryloxy, and methacryloxy.[31] However, KBM1803 did not show good adhesion strength despite containing double bonds. This is likely due to the long alkyl group in KBM1803 compared with other coupling agents. The long alkyl group reduces the possibility that the radicals from initiators will encounter double bonds in the coupling agent. The amino group and glycidyl do not produce good adhesion strength and it is probably because they do not produce radicals easily by the peroxide used in this study. We assessed the performance of the coupling agents with other mEPRs and found that KBM5103 showed the best results and was therefore employed it in subsequent experiments.

### Adhesion Strength of and Light Transmittance as a Function of SCA Content

Figure 4 shows the adhesion strength to the glass plate and the light transmittance of the EPR15 and EPR15/EPR9(5/5) blend as a function of the SCA content. The adhesion strength increased rapidly with the amount of SCA up to 1 phr, increased gradually up to 3 phr and leveled off with the further addition. The light transmittance did not change with the addition of the SCA up to 1 phr, decreased slowly up to 3 phr, and then dropped drastically with a further increase of SCA. Hence, we found that 1 phr of SCA is optimum content and therefore employed this concentration in subsequent experiments. It is seen that the adhesion strength of EPR15/EPR9(5/5) blend is slightly lower than that of EPR15. EPR9 shows nearly zero adhesion strength regardless of the SCA incorporation (not shown in Figure 4 for the space consideration). The pristine EPR15 and EPR9 show the adhesion strength of 9.4 and 0 N/cm, respectively, as shown in Table I. However the EPR15/EPR9(5/5) blend show slightly lower adhesion strength than that of EPR15 when the amount of SCA is over 1 phr. It is most likely that the grafting reaction occurs only between SCA and EPR15 (not EPR9 considering EPR9 shows nearly zero adhesion strength regardless of the SCA incorporation.). EPR15-g-SCA combines strongly EPR15/EPR9 blend and glass leading
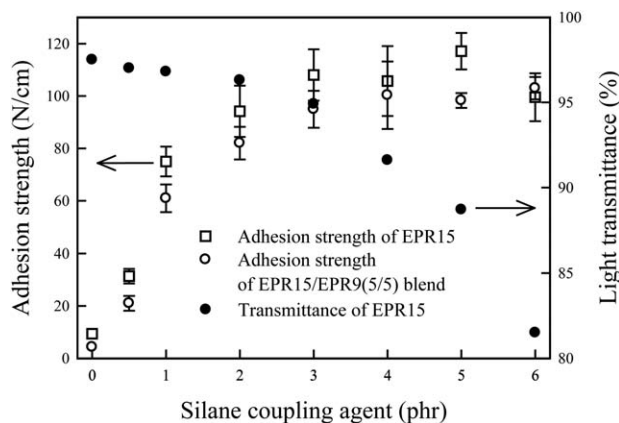


**Figure 4.** Adhesion strength and transmittance at 550 nm for EPR15 and EPR15/EPR9 (5/5) blend as a function of coupling agent content.

to strong adhesion because the EPR15 and EPR9 are miscible or at least strong interaction (as will be discussed in later section).

### Workability in Calendaring Process

The encapsulant preform is a thin film fabricated in a calendaring process. Although EPR15 and EPR16 show the highest light transmittances, adhesion strength and thermal creep resistances among the five polymers investigated, these two polymers show lower processability in a calendaring process. They adhere to the calendaring roller so much that the fabrication of a sheet is not possible. Altering the temperature and the roller speed provide only marginal improvement. Workability tests with the five mEPRs reveal that EPR with lower ethylene content does not have strong adherence to the roller.

Various combinations of resins were tested in terms of workability, thermal creep resistance, and adhesion strength. We found that the EPR15/EPR9(5/5) blend showed the best results except for light transmittance. The light transmittance of the EPR15/EPR9(5/5) blend was much lower than those of the pristine mEPRs (∼70%, as indicated in Figure 7). The EPR15/
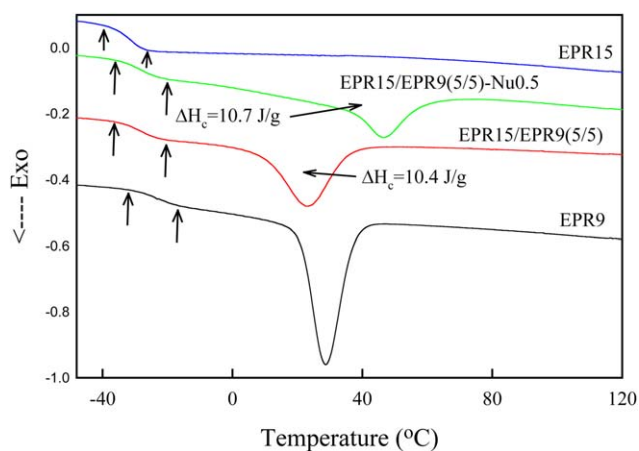


**Figure 5.** DSC cooling thermograms for EPR9, EPR15, and their blends. First, Samples were melted at 130 °C for 5 min, and a cooling scan was performed from 130 °C to −50 °C with a cooling rate of −20 °C/min. [Color figure can be viewed in the online issue, which is available at wileyonlinelibrary.com.]
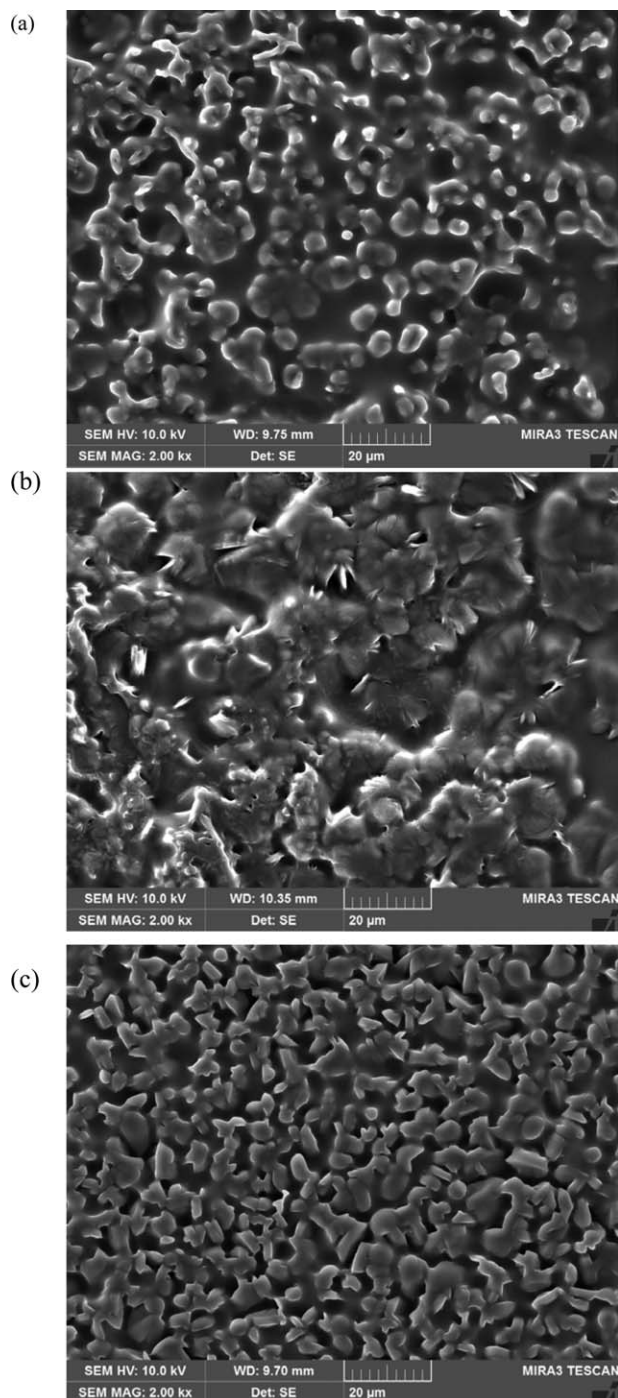
**Figure 6.** SEM micrograph for (a) EPR9, (b) EPR15/EPR9(5/5) and (c) EPR/15/EPR9(5/5)-Nu0.5.

EPR9(5/5) blend was transparent in the melt. However, the blend became turbid after it cooled down. Thus, it is likely that the turbidity is related to a crystallization behavior.

### Nucleation and Transparency of EPR15/EPR9(5/5) Blend

DSC cooling scan (Figure 5) shows that the crystallization peak temperature ($T_c$) and $T_g$ of EPR15/EPR9(5/5) is lower and the exotherm is broader compared to those of EPR9. If EPR15/EPR9(5/5) blend has a phase-separated and immiscible mor-

phology, both phases do not affect each other maintaining same $T_c$, $T_g$ and width of the exotherm. Thus, the depression of $T_c$ and $T_g$ indicate that EPR15 and EPR9 are miscible or at least partially miscible in a melt state. Depression of $T_c$ by addition of amorphous polymer or semi-crystalline polymer of the lower melting point have been used as an indication of miscibility or partial miscibility in many literatures.[33–35] Accordingly, the nucleation process of the EPR15/EPR9(5/5) blend is inferred to be slower than that of EPR9 (considering lowered $T_c$), leading to a lower number of nuclei and larger final spherulites. This was confirmed by SEM observation as shown in Figure 6. It is seen that EPR15/EPR9(5/5) blend shows bigger spherulites than those of EPR9. It has been reported that the transparency of a semi-crystalline polymer is mainly influenced by the size of the spherulite.[36–39] The bigger spherulites result in strong light scattering and poor transparency.[38,40] The size of the crystals have only marginal effects on the transparency.[38,40]

The light transmittance of the blend was greatly improved by the addition of a nucleating agent, as shown in Figure 7. The transmittance increased linearly by the addition of the nucleating agent, then leveled off and finally decreased with further addition. The nucleating agent increases the number of nuclei and enhances the nucleating process, leading to smaller spherulites and increased $T_c$. SEM observations reveal that the spherulite size of the blends is reduced by the addition of the nucleating agent, as shown in Figure 6. It is seen that 0.9 phr. of the nucleating agent provides the highest transmittance and further addition of the nucleating agent deteriorates the transparency. It is evident that an excess amount of additives scatters the light and reduces the light transmittance. It was also found that the adhesion strength of the EPR15/EPR9(5/5) blend was not affected by the nucleating agent. Though the nucleating agent reduced the size of the spherulites, the heat of crystallization (and consequently heat of fusion) were not affected by the nucleating agent as shown in Figure 5. As a consequence, the adhesion strength was not much affected by the existence of the nucleating agent.
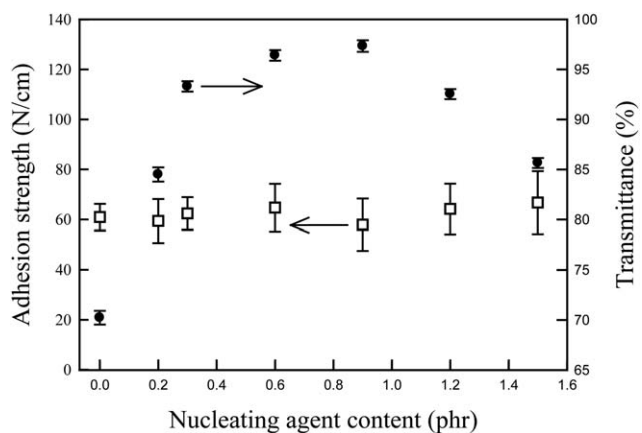


**Figure 7.** Average transmittance from 400 to 700 nm and adhesion strength for EPR15/EPR9(5/5) blend as a function of nucleating agent content. The blends were compounded with 1 phr of SCA, 0.06 phr of radical initiator and 0.2 phr of antioxidant.

## CONCLUSIONS

Five different EPRs having various ethylene and propylene content were investigated as encapsulants in a PV module. EPR with higher ethylene content led to higher transparency and higher adhesion strength to the glass plate. However, EPR with higher ethylene content led to lower processability in the calendaring process. Thus, a blend of EPR with the highest ethylene content and EPR with the lowest ethylene content was used as a base polymer for the encapsulant. When the two EPRs were blended, their transparency became lower than that of each component. This is due to the change of the spherulite size when the two different EPRs are mixed. Nucleating agents were incorporated in the blend of two EPRs and the transparency was remarkably increased. This is due to the decrease in the size of the spherulites. The adhesion strength to the glass plate was increased by SCAs.

## ACKNOWLEDGMENTS

## REFERENCES

1. Sun, S-S.; Sariciftci, N. S. Organic photovoltaics: mechanisms materials and devices; CRC Press: Boca Raton, **2005**.

2. Bube, R. H. Photovoltaic Materials; Imperial College Press: London, **1998**.

3. Amrani, A. E.; Mahrane, A.; Moussa, F. Y.; Boukennous, Y. *Int. J. Photoenergy* **2007**, *2007*.

4. Agroui, K.; Maallemia, A.; Boumaoura, M.; Collinsb, G.; Salama, M. *Sol. Energy Mater. Sol. Cells* **2006**, *90*, 2509.

5. Mishra, S. B.; Luyt, A. S. *J. Appl. Polym. Sci.* **2009**, *112*, 218.

6. Pern, F. J. U.S. Pat. 6093757 (2000).

7. Klemchuk, P.; Ezrin, M.; Lavigne, G.; Holley, W.; Galica, J.; Agro, S. *Polym. Degrad. Stab.* **1997**, *55*, 347.

8. Pern, F. J. *Angew Makromol. Chem* **1997**, *252*, 195.

9. Sultan, B. A.; Sorvik, E. *J. Appl. Polym. Sci.* **1991**, *43*, 1737.

10. Sultan, B. A.; Sorvik, E. *J. Appl. Polym. Sci.* **1991**, *43*, 1747.

11. Sultan, B. A.; Sorvik, E. *J. Appl. Polym. Sci.* **1991**, *43*, 1761.

12. Allen, N. S.; Edge, M.; Rodriguez, M.; Liauw, C. M.; Fontan, E. *Polym. Degrad. Stab.* **2000**, *68*, 363.

13. Kempe, M. D.; Jorgensen, G.; Terwilliger, K. M.; McMahon, T.; Kennedy, C. E.; Borek, T. T. *Sol. Energy Mater. Sol. Cells* **2007**, *91*, 315.

14. Hintersteiner, I.; Sternbauer, L.; Beissmann, S.; Buchberger, W.; Wallner, G.M. *Polym. Test.* **2014**, *33*, 172.

15. Ndiaye, A.; Charki, A.; Kobi, A.; Kébé, C.; Ndiaye, P. A.; Sambou, V. *Sol. Energy* **2013**, *96*, 140.

16. Armitage, J. B. U.S. Pat. 4351931 (1982).

17. Kim, N. S.; Han, C. W. *Sol. Energy Mater. Sol. Cells* **2013**, *116*, 68.

18. McNeill, I. C.; Mohammed, M. H. *Polym. Degrad. Stab.* **1995**, *48*, 175.

19. Jäger, K. M.; Dammert, R. C.; Sultan, B. A. *J. Appl. Polym. Sci.* **2002**, *84*, 1465.

20. Kempe, M. Proceedings of 37th IEEE Photovoltaic Specialists Conference **2011**, Seattle.

21. Hanoka, J. I. *U.S. Pat.* **2000**, 6114046 and 6353042.

22. Hanoka, J. I.; Klemchuk, P. P. *U.S. Pat.* **2002**, 6353042.

23. Holycross, M. E.; Saccocio, E. J. *U.S. Pat.* **1984**, 4474621.

24. Xie, Y.; Hill, C. A. S.; Xiao, Z.; Militz, H.; Mai, C. *Compos. Part A: Appl. Sci. Manuf.* **2010**, *41*, 806.

25. Chiang, W.; Yang, W. *J. Appl. Polym. Sci.* **1988**, *35*, 807.

26. Qiu, W.; Mai, K.; Zeng, H. *J. Appl. Polym. Sci.* **2000**, *77*, 2974. talc

27. Available at: http://rredc.nrel.gov/solar/old_data/nsrdb/1991-2005/tmy3/. Accessed on February 15, 2016.

28. Alamo, R. G.; Kim, M. H.; Galante, M. J.; Isasi, J. R.; Mandelkern, L. *Macromolecules* **1999**, *32*, 4050.

29. Auriemma, F.; De Rosa, C. *Macromolecules* **2002**, *35*, 9057.

30. Bruckner, S.; Meille, S. V.; Petraccone, V.; Pirozzi, B. *Prog. Polym. Sci.* **1991**, *16*, 361.

31. Assoun, L.; Manning, S. C.; Moore, R. B. *Polymer* **1998**, 2571.

32. Plueddemann, E. P. *J. Adhes.* **1970**, *22*, 184.

33. Hong, B. K.; Jo, W. H.; Kim, J. *Polymer* **1998**, *39*, 3753.

34. Chen, H.; Pyda, M.; Cebe, P. *Thermochim. Acta* **2009**, *492*, 61.

35. Huang, J.; Chang, F. *J. Appl. Polym. Sci.* **2002**, *84*, 850.

36. Zia, Q.; Androsch, R.; Radusch, H.-J. *J. Appl. Polym. Sci.* **2010**, *117*, 1013.

37. Lin, Y. J.; Dias, P.; Chum, S.; Hiltner, A.; Baer, E. *Polym. Eng. Sci* **2007**, *46*, 1658.

38. Mileva, D.; Androsch, R.; Radusch, H. *J. Polym. Bull.* **2009**, *62*, 561.

39. Shibayama, M.; Imamura, K. I.; Katoh, K.; Nomura, S. *J. Appl. Polym. Sci.* **1991**, *42*, 1451.

40. Gahleitner, M.; Grein, D.; Kheirandish, S.; Wolfschwenger, J. *Int. Polym. Process* **2011**, *26*, 2.